

Presented at the FIG Working Week 2019,
April 22-26, 2019 in Hanoi, Vietnam

ANALYSIS OF THE PERFORMANCE OF TWO GRAVIMETRIC REDUCTION SCHEMES

Abiodun, O. A ⁽¹⁾, Odumosu, J. O ⁽²⁾,
Oyekanbi, A. A ⁽²⁾ and Yusuff, S. F. ⁽²⁾

1. Department of surveying and Geoinformatics, Federal Polytechnic, Ado-Ekiti
2. Department of surveying and Geoinformatics, Federal University of Technology, Minna

ABSTRACT

Terrain correction (TC) in gravimetric reduction schemes is an essential component in gravimetric geoid modeling especially in areas with uneven topography. Two gravimetric reduction schemes (the second helmert's condensation method and the Rudzki's inversion method) are presented in this paper. A comparative analysis of the performance of the resulting anomalies from both schemes in relation to the study area's topography has also been evaluated. It was discovered that the Rudzki inversion produced a better statistical fit amongst the two reduction schemes although both methods produce similar terrain pattern when plotted in 2D across the study area. The study recommends that further investigations should be performed on the Rudzki inversion scheme

INTRODUCTION

▶ The classical solution of the geodetic BVP using Stokes's formula for geoid determination assumes that there should be no masses outside the geoid therefore, requiring a regularization of the actual earth's topography by some appropriate measures (Bajrachsharya, 2003). Classical terrain correction approach using the complete bouguer reduction assumes a constant bouguer slab and a correction term (Forsberg, 1985) and is as given by Heskanen and Moritz (1967) in equation 1

$$c_p = G \iiint_{E}^h \frac{\rho(x, y, z)(h_p - z)}{s^3(x_p - x, y_p - y, h_p - z)} d_x d_y d_z$$

Although the bouguer reduction produces smooth bouguer anomalies, it introduces a large indirect effect which makes it unsuitable for geoid modeling (Bajrachsharya, 2003). The Helmert's second method of condensation is therefore used as a practical means of gravimetric reduction scheme so as to minimize the indirect effect of topography on the geoid. In this scheme, the topographical masses are condensed on the geoid surface as a surface layer (Heck, 1999; Heck, 2003). The Rudzki inversion reduction scheme on the other hand is the only gravimetric reduction scheme which, by definition, does not change the equipotential surface and thus introduces zero indirect effect in geoid computation (Bajrachsharya and Sideris, 2004). In this method, the topographic masses above the geoid are inverted or mirrored into the interior of the geoid.

Several computational approaches have been developed based on equation (1) over the years using different mass models in both the spatial and spectral domain (Nagy, 1966; Blais and Ferland, 1984; Biagi and Sanso, 2001). Since the geoid is an equipotential surface of the earth's gravity field, the Ruzdki's reduction scheme tends to be theoretically appealing compared to the helmerts's condensation approach as it completely eliminates the indirect effect on the geoid. This paper presents a statistical comparison of Helmert and Ruzdki anomalies in the rugged topography of south western region of Nigeria.

HELMERT ANOMALY

▶ The Helmert anomaly is also called the Faye anomaly contains the high frequency part of the gravity signal representing the irregular part of the topography. It is the addition of Terrain correction (TC) to free air anomaly (Sideris, 1990) as mathematically described in equation (2) $\Delta g_{Faye} = FA + c$

▶ In the spectral domain, the Helmert's anomaly using a mass prism topographic model is given by Li and Sideris (1994) as equation (2)

$$\text{▶ } c_{1(i,j)} = \frac{G}{2} [(h_{ij}^2 - \alpha^2) \mathbf{F}^{-1}\{H_0 F_1\} - 2h_{ij} \mathbf{F}^{-1}\{H_1 F_1\} + \mathbf{F}^{-1}\{H_2 F_1\}] \quad (2a)$$

$$\text{▶ } c_{2(i,j)} = -\frac{G}{8} [(h_{ij}^2 - \alpha^2)^2 \mathbf{F}^{-1}\{H_0 F_2\} - 4h_{ij}(h_{ij}^2 - \alpha^2) \mathbf{F}^{-1}\{H_1 F_2\} + (6h_{ij}^2 - 2\alpha^2) \mathbf{F}^{-1}\{H_2 F_2\} - 4h_{ij} \mathbf{F}^{-1}\{H_3 F_2\} + \mathbf{F}^{-1}\{H_4 F_2\}]$$

(ZD)

Where:

$$\alpha = \frac{\sigma_h}{\sqrt{2}}$$

$$P = F(\rho), PH_1 = \mathbf{F}\{\rho h_{nm}\}, PH_2 = \mathbf{F}\{\rho h^2_{nm}\}, PH_3 = \mathbf{F}\{\rho h^3_{nm}\}, PH_4 = \mathbf{F}\{\rho h^4_{nm}\}$$

$$F_1 = \mathbf{F}\{f_{11}(x, y, \alpha) + f_{11}(y, x, \alpha) - f_{12}(x, y, \alpha)\}$$

$$F_2 = \mathbf{F}\{f_{21}(x, y, \alpha) + f_{21}(y, x, \alpha) - f_{22}(x, y, \alpha)\}$$

$$f_{11}(x, y, \alpha) = \frac{-x}{(y + r(x, y, \alpha)) \cdot r(x, y, \alpha)} \Big| \left\{ \begin{array}{l} x_n + \frac{\Delta x}{2} \\ \Delta x \end{array} \right\} \left\{ \begin{array}{l} y_n + \frac{\Delta y}{2} \\ \Delta y \end{array} \right\}$$

$$\blacktriangleright f_{22}(x, y, \alpha) = \frac{xy}{3(x^2y^2 + \alpha^2r^2)r} \cdot \left[\frac{2(r^2 + \alpha^2)^2}{(x^2y^2 + \alpha^2r^2)} - \frac{r^2}{\alpha^2} + \frac{r^2}{\alpha^2} - 4 \right] -$$

$$\frac{1}{3\alpha^3} \arctan \frac{xy}{\alpha r} \Big|_{\begin{matrix} x_n + \frac{\Delta x}{2} \\ x_n - \frac{\Delta x}{2} \end{matrix}}^{\begin{matrix} y_n + \frac{\Delta y}{2} \\ y_n - \frac{\Delta y}{2} \end{matrix}}$$

F and F^{-1} = fast Fourier transform and inverse Fourier respectively

Rudzki Anomalies

▶ Apart from Rudzki's own original work on this reduction scheme, it has not been used for geoid determination. Although, the method is purely mathematical and has no associated geophysical meaning, its limitation is not as important in geoid determination as in geophysics. A well studied derivation of its gravitational integrals can be seen in Bajrachsharya and Sideris (2004).

The expression for gravitational attraction due to the mass above the geoid is as given in (3) below:

$$A_p = 2\pi G\rho \left[h_p + a - \sqrt{a^2 + h_p^2} - G\rho \iint_E \left(\frac{1}{[s_0 + (h - h_p)^2]^{1/2}} \right) dE \right] \quad (3)$$

► The expression for the gravitational attraction at a point P on the topographical surface due to the mirrored topographical masses can also be expressed as a sum of the gravitational attraction due to regular and irregular parts of the inverted topography as equation (4):

$$A_p = 2\pi G\rho h_p - G\rho \iint_E \left(\frac{1}{[s_0 + (h_p - h)^2]^{1/2}} - \frac{1}{[s_0 + (h_p + h_p)^2]^{1/2}} \right) dE$$

(4)

Therefore, the expression for the direct topographical effect on gravity, which is equal to the difference between the gravitational attraction due to all topographical masses above the geoid and that due to the mirrored topographical masses inside the geoid in Rudzki's scheme, is as given below

$$\delta A_{Rudzki} = A_p - A = G\rho \iint_E \left(\frac{1}{s_0} - \frac{1}{[s_0 + (h - h_p)^2]^{1/2}} + \frac{1}{[s_0 + (h_p + h_p)^2]^{1/2}} - \frac{1}{[s_0^2 + (2h_p)^2]^{1/2}} \right) dE$$

Data Used

▶ Data used for this research is absolute gravity data observed using a simple pendulum device over some monumented horizontal control points within Minna metropolis. Orthometric heights of same points had already been established via spirit leveling and the values obtained from the office of the surveyor general of Niger state. The mean standard deviation of gravity observations across the stations used was 0.5mgals while the observational accuracy of the horizontal and vertical positions for the points were $\pm 0.008m$ and $\pm 0.053m$ respectively.

Results

Presented in Table 1 is the result of the Helmert and Rudzki anomalies at each of the observed stations while table 2 shows the statistics of the obtained gravity anomalies from both techniques. A graphical plot of the gravity anomalies as they cover the study area and their difference is presented in Figures 1a, b and c. Table 3 presents the results of a one-way ANOVA (analysis of variance) between the Rudzki and Faye anomaly.

Table 1: Numerical comparison of Faye and Rudzki anomalies

Station	East (m)	North (m)	Abs. Grav (mgals)	Ht (m)	Rudzki anor (mgals)	Helmert anor (mgals)	Diff
1	229205.836	1061834.490	980307.306	231.280	12.519	8.003	4.515
2	228250.090	1061503.286	979714.637	226.202	13.578	8.676	4.902
3	228080.712	1061440.132	980408.330	222.826	15.267	9.755	5.512
4	227783.051	1061338.595	980259.216	221.688	15.345	9.804	5.541
5	227311.464	1061111.394	978080.626	230.325	13.163	8.404	4.759
6	227105.006	1060924.058	978045.891	228.465	13.570	8.664	4.907
7	226924.900	1060721.579	979943.806	223.664	15.238	9.733	5.505
8	226487.377	1060263.575	979560.424	230.485	12.961	8.279	4.682
9	226359.804	1060123.522	979745.602	228.316	13.588	8.679	4.909
10	226002.705	1059747.275	980085.577	213.615	18.163	11.595	6.567
11	225566.036	1059285.935	978991.305	213.616	17.967	11.466	6.502
12	222087.338	1055238.513	978643.263	218.862	16.805	10.711	6.094
13	220563.819	1055093.113	980472.345	238.456	12.814	8.173	4.641

Table 2: statistics of gravity anomalies

	Max	Min	Mean	Stan Dev.	Range
Helmert	11.595	8.003	9.38	8.308	3.592
Rudzki	18.613	15.519	14.691	0.0000 002	3.094

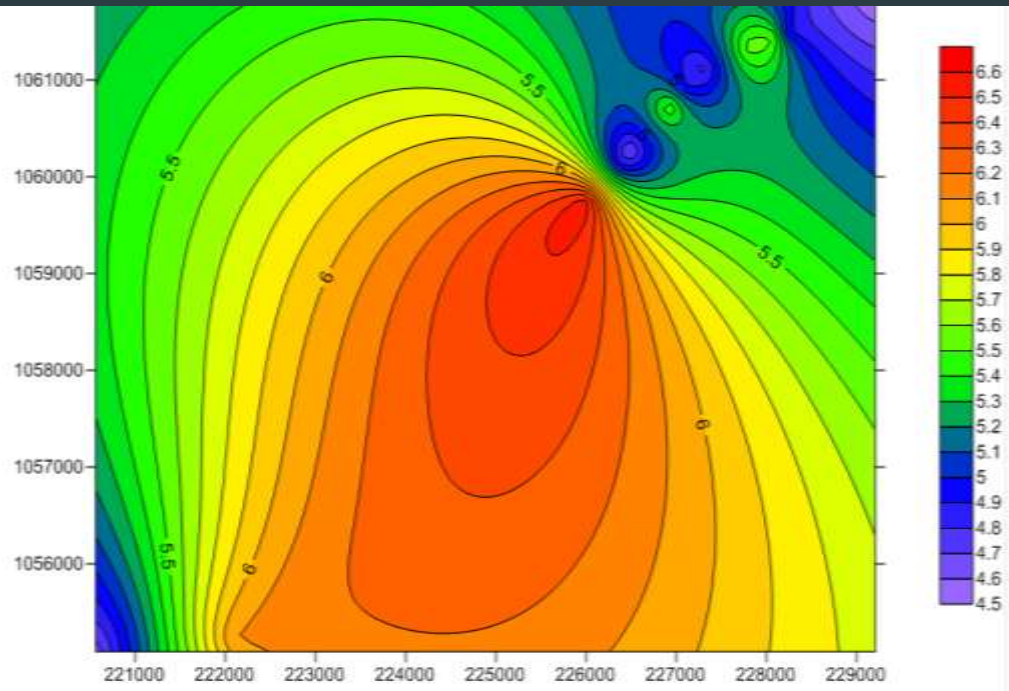
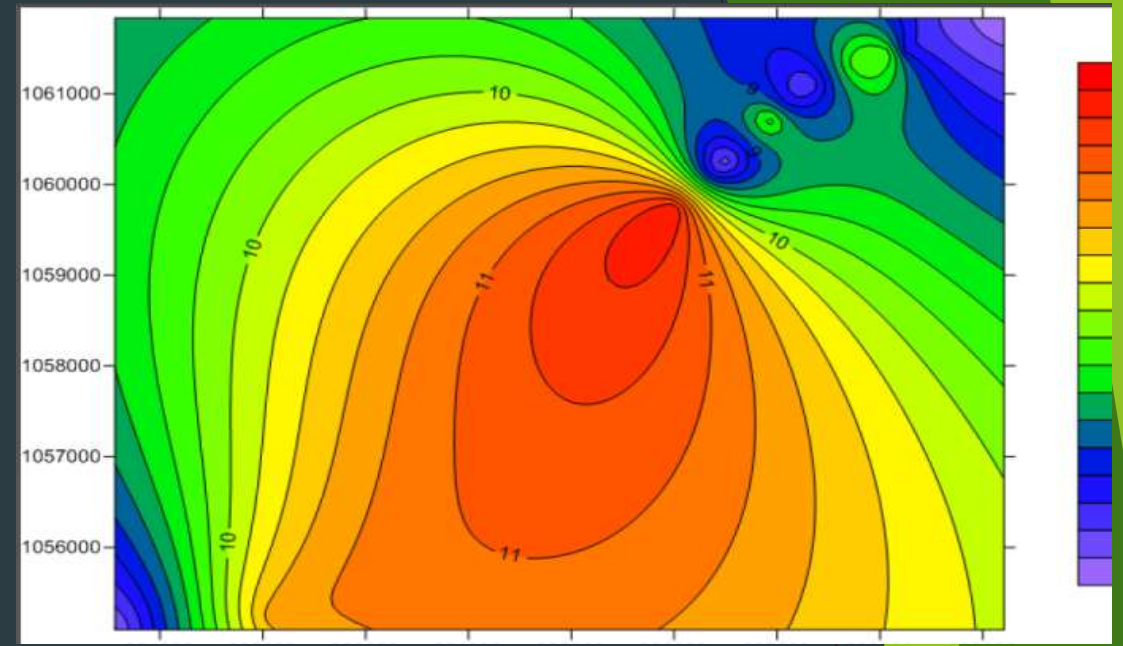
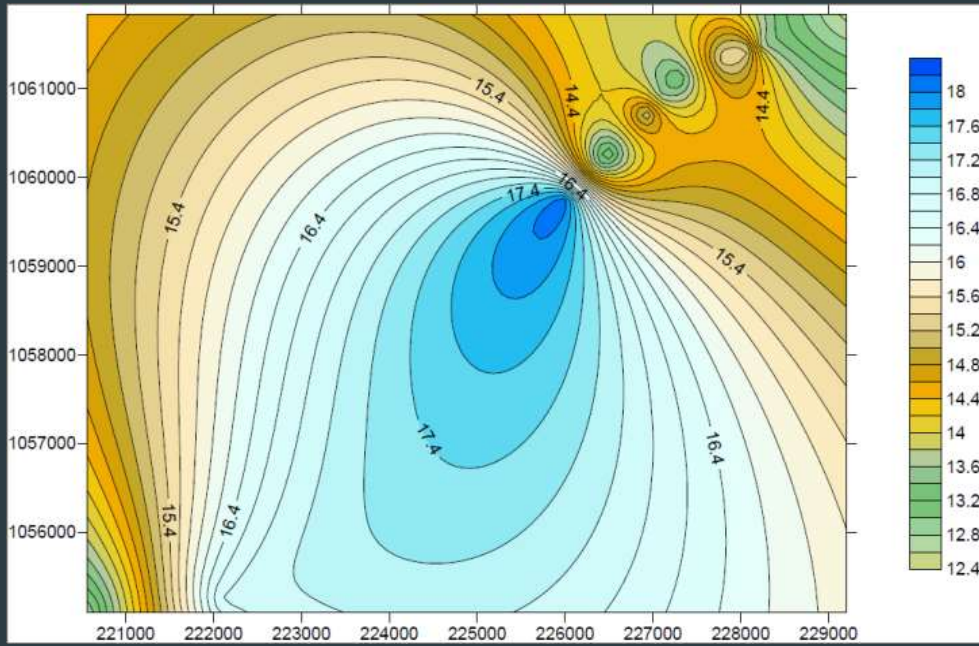


Figure 1(a): 2D Plot of Rudzki anomalies across study area.

Figure 1(b): 2D plot of Faye anomalies across the study area.

Anova: Single Factor

SUMMARY

<i>Groups</i>	<i>Count</i>	<i>Sum</i>	<i>Average</i>	<i>Variance</i>
<u>Rudzki ano</u> (mgals)	13	190.97719	14.69055	3.801
<u>Helmert ano</u> (mgals)	13	121.94061	9.380047	1.541

ANOVA

<i>Source of Variation</i>	<i>SS</i>	<i>df</i>	<i>MS</i>	<i>F</i>	<i>P-value</i>	<i>F crit</i>
Between Groups	183.3096	1	183.3096	68.65	0.00000002	4.259677214
Within Groups	64.089586	24	2.6703994			
Total	247.39918	25				

Figure 1(c): Plot of difference between Rudzki and Faye anomalies across study area

Figure 2 shows the correlation pattern between the two anomalies and the heights which is further supported by tables 4a and 4b.

Figure 2 shows the correlation pattern between the two anomalies and the heights which is further supported by tables 4a and 4b.

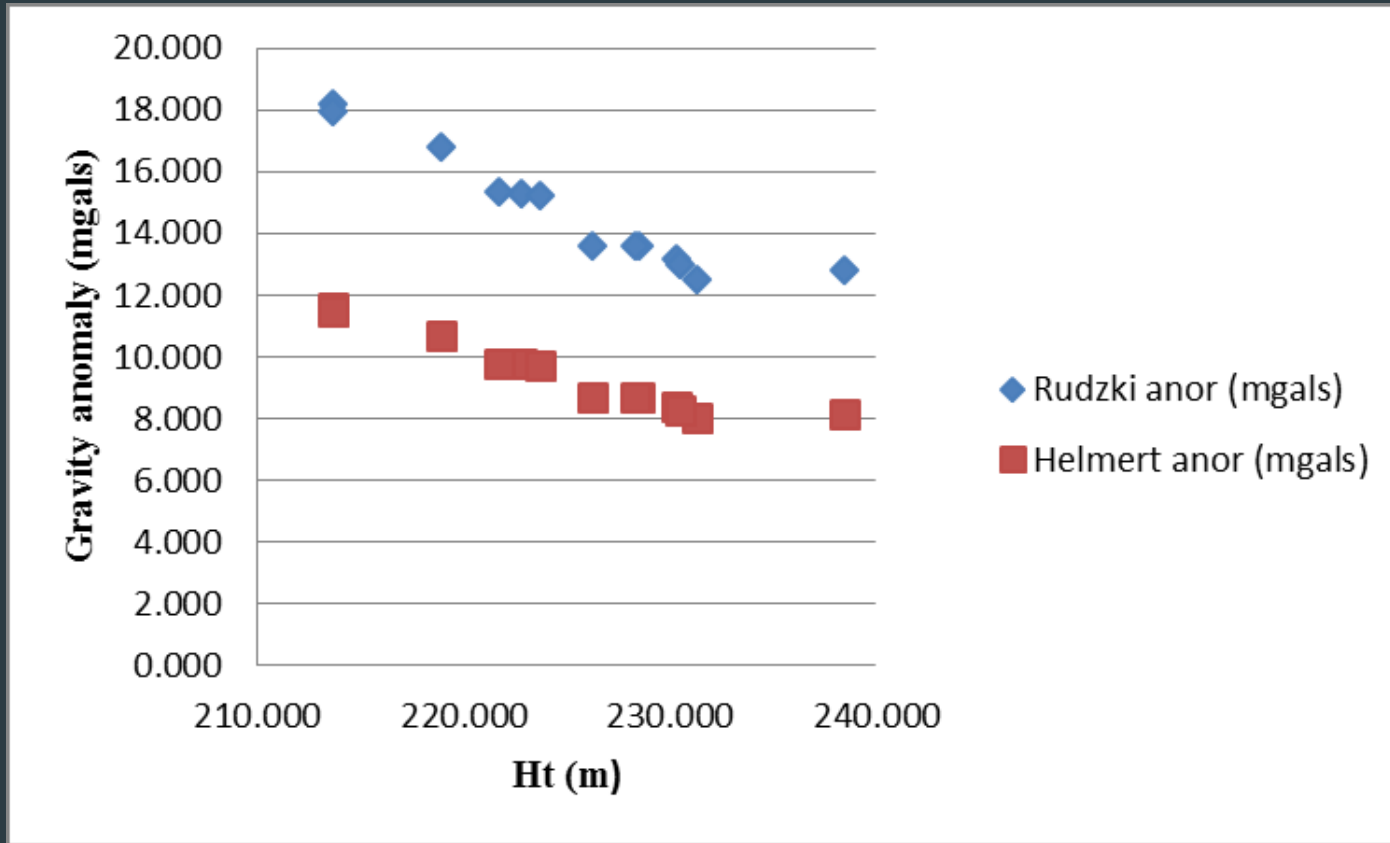


Figure 2: Correlation of the anomalies with topography.

Table 4a: Correlation Matrix between Rudzki anomaly and topography

	<i>Ht (m)</i>	<i>Rudzki ano (mgals)</i>
<i>Ht (m)</i>	1	-0.950
<i>Rudzki ano (mgals)</i>	-0.950	1

Table 4b: Correlation Matrix between Faye anomaly and topography

	<i>Ht (m)</i>	<i>Helmert ano (mgals)</i>
<i>Ht (m)</i>	1	-0.951
<i>Helmert ano (mgals)</i>	-0.951	1

Discussion of Results

▶ Although, the 2D plot of the Rudzki and Faye anomalies show similar pattern across the study area (Figure 1a - c) it is clearly visible from table 2 that the Rudzki inversion scheme produces better statistics compared to the Faye anomalies with smaller range and standard deviation of ± 0.00000002 mgals. The large parametric difference in values observed between both anomalies across the study area justifies the theoretical claim that the indirect effect is completely eliminated in the Rudzki inversion scheme.

The analysis of variance performed in table 3 shows that there is statistical significance between the means of the Rudzki and Faye anomalies. This is further justified by the observed difference in correlation pattern between the anomalies and the topography

Conclusion

In practical geoid determination using the remove-restore-compute (RRC) technique, the Faye anomaly is conventionally used with the indirect terrain effect applied during the restore process to compensate for the masses condensed during TC. The alternative use of the Rudzki anomalies has been investigated and the theoretical claim that it does not change the equipotential is herein confirmed. The similarity in the pattern of the 2D plot from both anomalies suggests the suitability of their interchangeable usage. Further investigations are recommended in further studies and in more rugged terrain.

REFERENCES

- Bajrachsharya, S. (2003). Terrain Effects on geoid determination. An MSc desertation of the department of Geomatics Engineering. University of Calgary.
- Bajrachsharya, S. and Sideris, M. G. (2004). The Rudzki inversion gravimetric reduction scheme in geoid determination. *Journal of Geodesy* (2004) 78. DOI: 10.1007/s00190-004-0397-y. Pgs 272 - 282.
- Biagi L and Sanso F. (2001) TcLight: a New technique for fast RTC computation. IAG Symposia, Vol. 123 Sideris (ed.), Gravity, Geoid, and Geodynamics 2000, Springer - Verlag Berlin Heidelberg 2001, pp 61-66.

Blais J. A. R. and Ferland R. (1984) Optimization in gravimetric terrain correction in western Canada. *Canadian Journal of Earth Sciences*, Vol.20, pp 259-265.

Forsberg, R (1985). Gravity Field Terrain Effect Computation by FFT. *Bulletin Geodesic* Vol.59, pp.342-360

Heck B. (1993) A revision of Helmert's second method of condensation in geoid and quasigeoid determination. In: Montag H, Reigber C (eds) *Geodesy and Physics of the Earth*. IAG Symposium no. 112. Springer, Berlin Heidelberg New York, pp 246-251

- ▶ Heck B. (2003) On Helmert's methods of condensation. *Journal of Geodesy* 77: 155-170.
- ▶ Heiskanen W. A, Moritz H. (1967). *Physical geodesy*. W. H. Freeman and Company. San Francisco.
- ▶ Li, Y. C and Sideris, M. G. (1994). Improved gravimetric terrain corrections. *Geophysics Journal International* 119, 740-752.
- ▶ Nagy D (1966) The prism method for terrain corrections using digital computers. *Pure Applied Geophysics*. Vol.63, pp 31-39
- ▶ Sideris, M. G. (1990). Rigorous Gravimetric terrain modeling using Molodensky's operator. *Manuscripta Geodaetica*, 15: 97-106.